

Power corrections to the process $\gamma^*\gamma \rightarrow \pi\pi$ in the running coupling method

S.S. Agaev^{1,2}, M. Guidal^{2,a}, B. Pire³

¹ High Energy Physics Laboratory, Baku State University, 370148 Baku, Azerbaijan

² Institut de Physique Nucléaire Orsay, 91406 Orsay, France

³ CPHT^b, École Polytechnique, 91128 Palaiseau, France

Received: 29 March 2004 / Revised version: 11 May 2004 /

Published online: 1 October 2004 – © Springer-Verlag / Società Italiana di Fisica 2004

Abstract. Power-suppressed corrections coming from the end-point integration regions in the amplitude of the process $\gamma^*\gamma \rightarrow \pi\pi$ at large Q^2 and small squared center-of-mass energy W^2 are calculated in the QCD hard-scattering approach where the amplitudes factorize in a hard perturbatively calculable part and a generalized distribution amplitude. The running coupling method and the technique of infrared renormalon calculus are applied to obtain Borel resummed expressions for the two main components of the process amplitude. Numerical estimates for these power corrections are presented. They are sizeable when $Q^2 < 10 \text{ GeV}^2$.

1 Introduction

Single meson and meson pair productions with a small invariant mass W in virtual photon–photon collisions are exclusive processes for which perturbative QCD (PQCD) [1] analysis was successfully applied when the virtuality Q^2 of one photon is high. These investigations are based on the perturbative QCD factorization theorems which allow one to compute the amplitude of the exclusive process as the convolution integral of the meson distribution amplitude (DA) or the two-meson generalized distribution amplitude (GDA) [2] and the hard-scattering amplitude of the underlying partonic subprocess. The meson DA's and GDA's $\phi(x, \mu_F^2)$ and $\phi(z, \zeta, W^2, \mu_F^2)$ are non-perturbative objects and contain the long-distance mesonic binding and hadronization effects. The GDA's are related by crossing [3] to the generalized parton distributions [4, 5]. The theoretical and experimental investigations of the processes $\gamma^*\gamma \rightarrow M\bar{M}$ open opportunities to obtain new, valuable information on the fragmentation of quarks or gluons into mesons [6]. These processes can be studied in $e\gamma$ and e^+e^- collisions and first results have been published [7].

The perturbative QCD approach and the factorization theorems describe exclusive processes at asymptotically large values of the squared momentum transfer Q^2 . But in the present experimentally accessible energy regimes, power-suppressed corrections may play an important role. There are numerous sources of power corrections to the process $\gamma^*\gamma \rightarrow M\bar{M}$. For example, power corrections arise due to the intrinsic transverse momentum of partons re-

tained in the corresponding subprocess hard-scattering amplitude and GDA's. They may be estimated along the lines presented in [8], where such corrections were calculated for the deeply virtual electroproduction of photon and mesons on the nucleon. A power correction to the process $\gamma^*\gamma \rightarrow \pi\pi$ has been estimated for the amplitude corresponding to scattering of two photons with equal helicities, with the help of the light-cone sum rules method [9]. The power-suppressed (twist-3) contribution due to the interaction of a longitudinally polarized virtual photon with the real one was analyzed within the Wandzura–Wilczek approximation in [10].

In the present paper we compute a class of power corrections which originate from the end-point regions $z \rightarrow 0, 1$ in the integration of the PQCD factorization expression over the parton longitudinal momentum fraction z . We restrict ourselves to the two-pion final state and to the leading twist-2 amplitudes. Generalization of our approach to encompass other two-meson final states is straightforward.

It has been advocated [11] that, in order to reduce the higher-order corrections to a physical quantity and improve the convergence of the corresponding perturbation series, the renormalization scale, i.e. the argument of the QCD coupling in a Feynman diagram should be set equal to the virtual parton's squared four-momentum. In exclusive processes, the scale chosen this way inevitably depends on the longitudinal momentum fractions carried by the hadron constituents. In our case, the relevant scale is given by $\mu_R^2 = Q^2 z$ or $Q^2 \bar{z}$ [2]. But then the PQCD factorization formula diverges, since $\alpha_s(Q^2 z)$ [$\alpha_s(Q^2 \bar{z})$] suffers from an end-point $z \rightarrow 0$ [$z \rightarrow 1$] singularity. This prob-

^a e-mail: guidal@ipno.in2p3.fr

^b Unité mixte de recherche du CNRS (UMR 7644).

lem may be solved by freezing the argument of the QCD coupling and performing all calculations with $\alpha_s(Q^2)$ [or $\alpha_s(Q^2/2)$]. In the running coupling (RC) method, one allows the argument of α_s to run but removes divergences appearing in the perturbative expression with the help of a Borel transformation and a principal value prescription. It turns out that this procedure, used in conjunction with the infrared (IR) renormalon technique [12,13] allows one to obtain the Borel resummed expression for the process amplitude and estimate power corrections arising from the end-point integration regions. This method was used for other processes [14–18] and successfully confronted to experimental data.

This paper is organized as follows: in Sect. 2 we present kinematics, general expressions for the amplitude of the process and the two-pion GDA's. In Sect. 3 we outline the main points of the RC method and obtain the Borel resummed components of the amplitude. Section 4 contains results of our numerical calculations. Finally, we give our conclusions in Sect. 5.

2 Amplitude of the process $\gamma^*\gamma \rightarrow \pi\pi$

The process

$$\gamma^*(q) + \gamma(q') \rightarrow \pi(p_1) + \pi(p_2), \quad (1)$$

is schematically depicted in Fig. 1. In addition to the four-momenta of the initial and final particles one introduces the total and relative momenta of the pion pair $P = p_1 + p_2$, $\Delta = p_2 - p_1$. The momenta of the involved particles can be described in terms of two light-like vectors p , n which obey $p \cdot n = 1$. The decomposition of the four-momenta of the initial and final states in terms of the vectors p and n reads

$$q = p - \frac{Q^2}{2}n, \quad q' = \frac{Q^2 + W^2}{2}n, \quad q^2 = -Q^2, \quad q'^2 = 0,$$

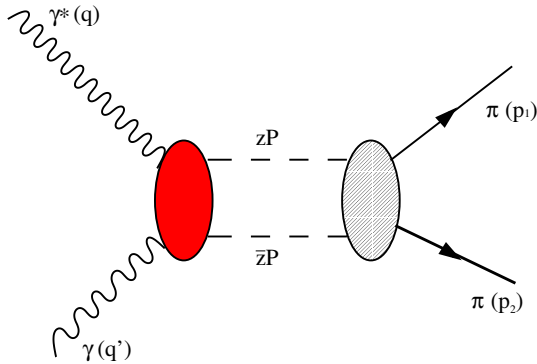


Fig. 1. Schematic representation of the factorization theorem for the process $\gamma^*\gamma \rightarrow \pi\pi$. The solid and dashed blobs denote the hard-scattering subprocess $\gamma^*\gamma \rightarrow q\bar{q}$ ($\gamma^*\gamma \rightarrow gg$) and hadronization $q\bar{q} \rightarrow \pi\pi$ ($gg \rightarrow \pi\pi$), respectively. The quarks (gluons) are depicted as dashed lines. The momenta of the initial and final particles are shown in the figure. The total momentum of the final state is $P = p_1 + p_2$ and z is the longitudinal momentum fraction of the 2π system carried by the quark (gluon)

$$\begin{aligned} p_1 &= \zeta p + \bar{\zeta} \frac{W^2}{2}n - \frac{k_\perp}{2}, \quad p_2 = \bar{\zeta} p + \zeta \frac{W^2}{2}n + \frac{k_\perp}{2}, \\ P &= p + \frac{W^2}{2}n, \quad P^2 = W^2, \\ \Delta &= (\bar{\zeta} - \zeta)p + (\zeta - \bar{\zeta}) \frac{W^2}{2}n + k_\perp, \end{aligned} \quad (2)$$

where the quantities

$$\zeta = \frac{p_1 \cdot n}{P \cdot n}, \quad \bar{\zeta} = 1 - \zeta = \frac{p_2 \cdot n}{P \cdot n},$$

describe the distribution of the longitudinal momentum between two pions. The vectors p and n can also be employed to define the metric tensor in the transverse space:

$$(-g^{\mu\nu})_T = -g^{\mu\nu} + p^\mu n^\nu + p^\nu n^\mu. \quad (3)$$

In the hard photoproduction regime $Q^2 \gg W^2, \Lambda^2$ the amplitude of the process (1) has the form

$$\begin{aligned} T^{\mu\nu}(\zeta, W^2) &= \frac{i}{2} (-g^{\mu\nu})_T T_0(\zeta, W^2) \\ &+ \frac{i}{2} \frac{k_\perp^\mu (P + q')^\mu}{Q^2} T_1(\zeta, W^2) + \frac{i}{2} \frac{k_\perp^{(\mu} k_\perp^{\nu)}}{W^2} T_2(\zeta, W^2), \end{aligned} \quad (4)$$

where $k_\perp^{(\mu} k_\perp^{\nu)}$ is the traceless, symmetric tensor product of the relative transverse momentum of the pion pair

$$k_\perp^{(\mu} k_\perp^{\nu)} = k_\perp^\mu k_\perp^\nu - \frac{1}{2} (-g^{\mu\nu})_T k_\perp^2.$$

In (4) $T_0(\zeta, W^2)$ is the amplitude corresponding to the scattering of two photons with equal helicities, $T_1(\zeta, W^2)$ denotes the amplitude with $L_z = \pm 1$, whereas $T_2(\zeta, W^2)$ arises from the subprocess with opposite helicity photons. In fact, in the collinear approximation, conservation of the angular momentum along the collision axis leads to the helicity conservation $h^* - h = h_1 + h_2$, where h^* , h are the helicities of the virtual and real photons and h_1 , h_2 denote the helicities of the produced quarks or gluons. When photons produce a quark–antiquark pair, at the leading twist-2 level only the subprocess with $L_z = 0$ contributes to the amplitude. The subprocess with $L_z = \pm 1$ is twist-3 and determines the contribution $T_1(\zeta, W^2)$ appearing due to the interaction of a longitudinally polarized virtual photon with the real one [10]. In the case where photons create a gluon pair, both the subprocesses with $L_z = 0$ and $L_z = \pm 2$ contribute at the twist-2 level to (4).

We now focus on the amplitudes $T_i(\zeta, W^2)$, $i = 0, 2$, which do not vanish at leading twist. They can be written as convolution integrals of hard-scattering coefficient functions $C(z, \mu_F^2)$ and two-pion GDA's $\Phi(z, \zeta, W^2, \mu_F^2)$, i.e.

$$\begin{aligned} T_0(\zeta, W^2) &= \sum e_q^2 \int_0^1 dz C_q(z, \mu_F^2) \Phi_q(z, \zeta, W^2, \mu_F^2) \\ &- \sum e_q^2 \int_0^1 dz C_g(z, \mu_F^2) \Phi_g(z, \zeta, W^2, \mu_F^2) \end{aligned} \quad (5)$$

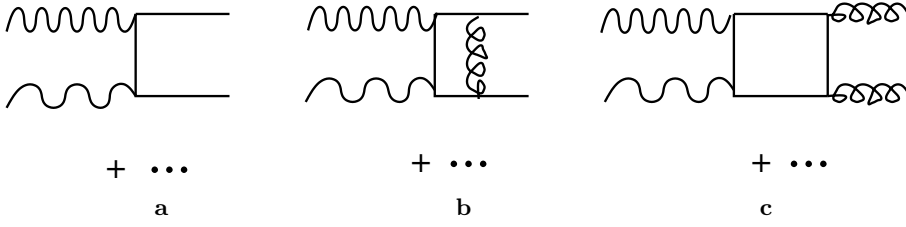


Fig. 2. Sample Feynman diagrams of the hard-scattering subprocesses $\gamma^*\gamma \rightarrow q\bar{q}$ (at leading order – **a**, at next-to-leading order – **b**) and $\gamma^*\gamma \rightarrow gg$ (**c**)

and

$$T_2(\zeta, W^2) = \int_0^1 dz C_g^T(z, \mu_F^2) \Phi_g^T(z, \zeta, W^2, \mu_F^2), \quad (6)$$

where μ_F^2 is the factorization scale at which the hard and soft parts of the reaction are defined. Here the coefficient function $C_q(z, \mu_F^2)$ is calculated with NLO accuracy using the subprocess $\gamma^*\gamma \rightarrow q\bar{q}$ (Fig. 2a,b) with $L_z = 0$, whereas the functions $C_g(z, \mu_F^2)$ and $C_g^T(z, \mu_F^2)$ correspond to the subprocess $\gamma^*\gamma \rightarrow gg$ (Fig. 2c) with $L_z = 0$ and $L_z = \pm 2$, respectively, and contribute only at the next-to-leading order of PQCD due to quark-box diagrams.

The amplitudes $T_i(\zeta, W^2)$ do not depend on the renormalization and factorization schemes and scales employed for their calculation. But at any finite order of QCD perturbation theory, due to truncation of the corresponding perturbation series, the coefficient functions depend on both the factorization μ_F^2 and renormalization μ_R^2 scales. An optimal choice for these scales is always required to minimize higher-order corrections. The factorization scale μ_F^2 in exclusive processes is traditionally set equal to the hard momentum transfer Q^2 , and we shall follow this prescription.

The functions $C(z)$ with NLO accuracy are given by the following expressions [19]:

$$C_q(z) = C_q^0(z) + \frac{\alpha_s(\mu_R^2)}{4\pi} C_q^1(z), \quad (7)$$

$$C_g(z) = \frac{\alpha_s(\mu_R^2)}{4\pi} C_g^1(z),$$

$$C_g^T(z) = \frac{\alpha_s(\mu_R^2)}{4\pi} C_T^1(z), \quad (8)$$

and

$$\begin{aligned} C_q^0(z) &= \frac{1}{\bar{z}} - \frac{1}{z}, \\ C_q^1(z) &= C_F \left[\frac{\ln^2 \bar{z}}{z\bar{z}} - \frac{\ln^2 z}{z\bar{z}} + \frac{\ln^2 z}{\bar{z}} - \frac{\ln^2 \bar{z}}{z} + 3 \frac{\ln z}{\bar{z}} \right. \\ &\quad \left. - 3 \frac{\ln \bar{z}}{z} + \frac{9}{z} - \frac{9}{\bar{z}} \right], \\ C_g^1(z) &= \frac{1}{z^2 \bar{z}^2} [z^2 \ln^2 z + \bar{z}^2 \ln^2 \bar{z} + 2z\bar{z} \ln z \bar{z} \\ &\quad - 4z \ln z - 4\bar{z} \ln \bar{z}], \\ C_T^1(z) &= \frac{2}{z\bar{z}}, \end{aligned} \quad (9)$$

with $C_F = 4/3$ being the color factor.

Choosing the renormalization scale μ_R^2 is more subtle and we follow the prescription [11] that it is equal to the square of the momentum transfer carrying by a virtual parton in each leading order Feynman diagram of the underlying hard-scattering subprocess. Here, these scales are determined by the leading order diagrams of the subprocess $\gamma^*\gamma \rightarrow q\bar{q}$ and are given by the virtualities of the off-shell fermion, which are equal to $Q^2 z$ or to $Q^2 \bar{z}$ depending on the diagram. In the present paper we adopt the symmetrized RC method, where $\alpha_s(Q^2 z)$ and $\alpha_s(Q^2 \bar{z})$ are replaced by

$$\alpha_s(Q^2 z), \alpha_s(Q^2 \bar{z}) \Rightarrow \frac{\alpha_s(Q^2 z) + \alpha_s(Q^2 \bar{z})}{2}. \quad (10)$$

The reasons which led to introduction of this version of the RC method and further details have been presented in [17,18].

The next component in the factorization formulas (5), (6) is the generalized distribution amplitudes of the 2π system. At present, little is known about these GDA's, but using constraints originating from crossing symmetry and soft pion theorems, as well as the evolution equation for GDA's, we can model them. Further information on their analytic form should be extracted from analysis of experimental data and corresponding theoretical predictions and/or obtained, as in the case of the usual DA's of mesons, via QCD non-perturbative methods.

The simplest 2π GDA's obtained using the requirements described above are

$$\Phi_q(z, \zeta, W^2, \mu_F^2) = 20z\bar{z}(z - \bar{z}) \frac{1}{n_f} M_q(\mu_F^2) A(\zeta, W^2),$$

$$\Phi_g(z, \zeta, W^2, \mu_F^2) = 10z^2 \bar{z}^2 M_g(\mu_F^2) A(\zeta, W^2), \quad (11)$$

where the model-dependent [20] function $A(\zeta, W^2)$ is z and Q^2 independent. Our results will not depend on the choice of this function.

The GDA's represented by the formula (11) depend on the momentum fractions carried by quarks $M_q(\mu_F^2)$ and gluons $M_g(\mu_F^2)$ in the pion

$$M_q(\mu_F^2) = M_q^{\text{asy}} \{1 + R(\mu_0^2) L(\mu_F^2)\},$$

$$R(\mu_0^2) = \frac{M_q(\mu_0^2) - M_q^{\text{asy}}}{M_q^{\text{asy}}},$$

with

$$\begin{aligned} L(\mu_F^2) &= \left[\frac{\alpha_s(\mu_F^2)}{\alpha_s(\mu_0^2)} \right]^{\frac{\gamma_1^+}{\beta_0}}, \quad \gamma_1^+ = \frac{2}{3}(n_f + 4C_F), \\ M_g(\mu_F^2) &= 1 - M_q(\mu_F^2), \end{aligned} \quad (12)$$

the asymptotic values of which are determined by the expressions

$$M_q^{\text{asy}} = \frac{n_f}{n_f + 4C_F}, \quad M_g^{\text{asy}} = \frac{4C_F}{n_f + 4C_F}. \quad (13)$$

For the helicity-two GDA $\Phi_g^T(z, \zeta, W^2, \mu_F^2)$ we take

$$\Phi_g^T(z, \zeta, W^2, \mu_F^2) = D(\mu_F^2) z^2 \bar{z}^2 A_g^T(\zeta, W^2), \quad (14)$$

with

$$D(\mu_F^2) = 30 D_g^T(\mu_0^2) \left[\frac{\alpha_s(\mu_F^2)}{\alpha_s(\mu_0^2)} \right]^{\frac{\gamma^{\text{TG}}}{\beta_0}}, \quad (15)$$

$$\gamma^{\text{TG}} = 7 + \frac{2}{3} n_f.$$

In (12) and (15) μ_0^2 and $D_g^T(\mu_0^2)$ are the normalization point and constant, respectively.

3 Borel resummed amplitudes

Computation of the amplitudes $T_i(Q^2, \zeta, W^2)$ implies integrations over z . Having inserted the explicit expressions of the hard-scattering coefficient functions and the two-pion GDA's into (5) and (6) we encounter divergences, arising from the singularities of the coupling constant $\alpha_s(Q^2 z)$ and $\alpha_s(Q^2 \bar{z})$ in the limits $z \rightarrow 0, 1$. The RC method proposes a way to cure these divergences.

To this end we express the running coupling $\alpha_s(Q^2 z)$ in terms of $\alpha_s(Q^2)$ [a similar argument holds also for $\alpha_s(Q^2 \bar{z})$]. This is achieved by applying the renormalization-group equation to $\alpha_s(Q^2 z)$ [21]. We get

$$\alpha_s(Q^2 z) \simeq \frac{\alpha_s(Q^2)}{1 + \frac{\ln z}{t}} \left[1 - \frac{\alpha_s(Q^2) \beta_1 \ln \left[1 + \frac{\ln z}{t} \right]}{2\pi\beta_0 \left(1 + \frac{\ln z}{t} \right)} \right]. \quad (16)$$

Here $\alpha_s(Q^2)$ is the one-loop QCD coupling constant, $t = 4\pi/\beta_0 \alpha_s(Q^2) = \ln(Q^2/\Lambda^2)$ and β_0, β_1 are the QCD beta function one- and two-loop coefficients, respectively,

$$\beta_0 = 11 - \frac{2}{3} n_f, \quad \beta_1 = 51 - \frac{19}{3} n_f,$$

and n_f is the number of active quark flavors. Equation (16) expresses $\alpha_s(Q^2 z)$ in terms of $\alpha_s(Q^2)$ with an $\alpha_s^2(Q^2)$ order accuracy.

Inserting (16) into the amplitudes we obtain integrals, which can be regularized and calculated using the method described in [14]. The amplitudes $T_i(Q^2, \zeta, W^2)$ are then written as perturbative series in $\alpha_s(Q^2)$ with factorially growing coefficients $C_n \sim (n-1)!$. Their resummation is performed by employing the Borel integral technique [22]. Namely, one has to determine the Borel transforms $B[T_i(Q^2, \zeta, W^2)](u)$ of the corresponding series and in order to find the resummed expression for the amplitudes, has to invert $B[T_i(Q^2, \zeta, W^2)](u)$ to get

$$\begin{aligned} & [T_i(Q^2, \zeta, W^2)]^{\text{res}} \\ & \sim \text{P.V.} \int_0^\infty du \exp \left[-\frac{4\pi u}{\beta_0 \alpha_s(Q^2)} \right] B[T_i(Q^2, \zeta, W^2)](u) \\ & \quad + [T_i(Q^2, \zeta, W^2)]^{\text{amb}} \end{aligned} \quad (17)$$

The Borel transforms $B[T_i(Q^2, \zeta, W^2)](u)$ contain poles $\{u_0\}$ located at the positive u axis of the Borel plane, which are exactly the IR renormalon poles. Therefore, the inverse Borel transformation can be computed after regularization of these pole singularities, which is achieved through a principal value prescription. But the principal value prescription itself generates higher twist (HT) ambiguities (uncertainties), which in the right-hand side of (17) are denoted by $[T_i(Q^2, \zeta, W^2)]^{\text{amb}}$. They are determined by the residues of the Borel transforms at the IR renormalon poles $q \in \{u_0\}$ and depend also on unknown numerical coefficients $\{N_q\}$

$$[T_i(Q^2, \zeta, W^2)]^{\text{amb}} \sim \sum_{q \in \{u_0\}} N_q \frac{\Phi_i^q(Q^2, \zeta, W^2)}{Q^{2q}}. \quad (18)$$

The ambiguity (18) can be used to estimate higher twist corrections to the amplitudes stemming from other sources [for example, from the 2π higher twist GDA's].

A useful way to avoid the intermediate operations and obtain directly the Borel resummed expressions is to introduce the inverse Laplace transformations of the functions in (16), i.e.

$$\frac{1}{(t+x)^\nu} = \frac{1}{\Gamma(\nu)} \int_0^\infty du \exp[-u(t+x)] u^{\nu-1}, \quad \text{Re} \nu > 0, \quad (19)$$

and

$$\frac{\ln[t+x]}{(t+x)^2} = \int_0^\infty du \exp[-u(t+x)] (1 - \gamma_E - \ln u) u, \quad (20)$$

where $\Gamma(\nu)$ is the Gamma function, $\gamma_E \simeq 0.577216$ is the Euler constant and $x = \ln z$ [$x = \ln \bar{z}$ in the case $\alpha_s(Q^2 \bar{z})$]. Then, the QCD coupling $\alpha_s(Q^2 z)$ may be written as [16]

$$\alpha_s(Q^2 z) = \frac{4\pi}{\beta_0} \int_0^\infty du e^{-ut} R(u, t) z^{-u}, \quad (21)$$

with

$$R(u, t) = 1 - \frac{2\beta_1}{\beta_0^2} u (1 - \gamma_E - \ln t - \ln u). \quad (22)$$

The expression for the QCD running coupling (21) is obtained from (16) and is suited to account for the end-point effects. It differs from that introduced to perform the resummation of diagrams with quark vacuum insertions ("bubble chains") into a gluon line [12, 13]. In exclusive processes both these sources lead to power corrections. As noted above, in the present work we consider contributions to the process amplitudes arising only from the end-point regions.

Using (11), (14) and (21) and performing the integration over z we get¹

$$[T_0(Q^2, \zeta, W^2)]^{\text{res}} = 20A(\zeta, W^2) \times \sum e_q^2 \left\{ \frac{M_q(Q^2)}{3n_f} \left[1 + \frac{3C_F}{\beta_0} \int_0^\infty du e^{-ut} R(u, t) Q(u) \right] - \frac{M_g(Q^2)}{2\beta_0} \int_0^\infty du e^{-ut} R(u, t) G(u) \right\}, \quad (23)$$

and

$$[T_2(Q^2, \zeta, W^2)]^{\text{res}} = 2A_g^T(\zeta, W^2) \frac{D(Q^2)}{\beta_0} \times \int_0^\infty du e^{-ut} R(u, t) B(2-u, 2), \quad (24)$$

with

$$Q(u) = \frac{\partial^2}{\partial \beta^2} B(2-u, \beta)|_1 + \frac{d^2}{d\beta^2} B(2, \beta)|_{1-u} - \frac{\partial^2}{\partial \beta^2} B(1-u, \beta)|_2 - \frac{d^2}{d\beta^2} B(1, \beta)|_{2-u} + \frac{\partial^2}{\partial \beta^2} B(1-u, \beta)|_3 + \frac{d^2}{d\beta^2} B(1, \beta)|_{3-u} - \frac{\partial^2}{\partial \beta^2} B(2-u, \beta)|_2 - \frac{d^2}{d\beta^2} B(2, \beta)|_{2-u} + 3 \frac{\partial}{\partial \beta} B(1-u, \beta)|_3 + 3 \frac{d}{d\beta} B(1, \beta)|_{3-u} - 3 \frac{\partial}{\partial \beta} B(2-u, \beta)|_2 - 3 \frac{d}{d\beta} B(2, \beta)|_{2-u} - 9B(3-u, 1) - 9B(1-u, 3) + 18B(2-u, 2) \quad (25)$$

and

$$G(u) = \frac{\partial^2}{\partial \beta^2} B(1-u, \beta)|_3 + \frac{d^2}{d\beta^2} B(1, \beta)|_{3-u} + 2 \frac{\partial}{\partial \beta} B(2-u, \beta)|_2 + 2 \frac{d}{d\beta} B(2, \beta)|_{2-u} - 4 \frac{\partial}{\partial \beta} B(1-u, \beta)|_2 - 4 \frac{d}{d\beta} B(1, \beta)|_{2-u}, \quad (26)$$

where $B(x, y)$ is the Beta function $B(x, y) = \Gamma(x)\Gamma(y)/\Gamma(x+y)$.

In order to proceed one has to reveal the IR renormalon poles in the resummed expressions. The analysis of the pole structure of $Q(u)$ and $G(u)$ is straightforward. The result is that the function $Q(u)$ contains a finite number of triple poles located at $u_0 = 1, 2, 3$, an infinite number of double poles at the points $u_0 = 2, 3, 4 \dots \infty$ and single ones at the points $u_0 = 1, 2, 3, 4 \dots \infty$. For the function $G(u)$ we get: triple pole with location at $u_0 = 3$, infinite number of double ($u_0 = 2, 3, 4 \dots \infty$) and single poles ($u_0 = 1, 2, 3, 4 \dots \infty$). The amplitude $[T_2(Q^2, \zeta, W^2)]^{\text{res}}$

possesses only single poles at $u_0 = 2, 3$. In other words, by employing (16) we have transformed the end-point divergences in (5) and (6) into the IR renormalon pole divergences in (23) and (24). One can see that the integrals in these expressions are the inverse Borel transformations (17), where the Borel transforms $B_{q(g)}[T_0(Q^2, \zeta, W^2)](u)$ of the quark and gluon components of the amplitude $[T_0(Q^2, \zeta, W^2)]^{\text{res}}$ (in the quark case the NLO part) and that of the amplitude $[T_2(Q^2, \zeta, W^2)]^{\text{res}}$ up to constant factors are defined as

$$B_{q(g)}[T_0(Q^2, \zeta, W^2)](u) \sim R(u, t) Q(u) [-G(u)], \\ B[T_2(Q^2, \zeta, W^2)](u) \sim R(u, t) B(2-u, 2).$$

After removing IR renormalon divergences from (23) and (24) by means of the principal value prescription, they determine the resummed amplitudes $[T_i(Q^2, \zeta, W^2)]^{\text{res}}$. The final expressions $[T_i(Q^2, \zeta, W^2)]^{\text{res}}$ contain power-suppressed corrections $\sim 1/Q^{2n}$, $n = 1, 2, 3, \dots$ to the amplitudes [16–18] and are the main results of the present work.

Let us now check the asymptotic limit of the resummed amplitudes. In the asymptotic limit $Q^2 \rightarrow \infty$, GDA's $\Phi_q(z, \zeta, W^2, Q^2)$ and $\Phi_g(z, \zeta, W^2, Q^2)$ evolve to their asymptotic forms obtainable from (11) by means of the replacements $M_q(Q^2) \rightarrow M_q^{\text{asy}}$ and $M_g(Q^2) \rightarrow M_g^{\text{asy}}$. We need also to take into account that in this limit the subleading term in the expansion of $\alpha_s(Q^2 z)$ through $\alpha_s(Q^2)$ should be neglected, i.e.

$$\int_0^\infty du e^{-ut} R(u, t) \rightarrow \int_0^\infty du e^{-ut}. \quad (27)$$

Then the amplitude $[T_0(Q^2, \zeta, W^2)]^{\text{res}}$ takes the following form:

$$[T_0(Q^2, \zeta, W^2)]^{\text{res}} = \frac{20A(\zeta, W^2)}{3(n_f + 4C_F)} \times \sum e_q^2 \left\{ 1 + \frac{3C_F}{\beta_0} \int_0^\infty du e^{-ut} [Q(u) - 2G(u)] \right\}. \quad (28)$$

The asymptotic limit of the integrals can be computed using techniques, described in a detailed form in [17, 18]. After some manipulations, one gets for the asymptotic limit of the amplitude $[T_0(Q^2, \zeta, W^2)]^{\text{res}}$

$$[T_0(Q^2, \zeta, W^2)]^{\text{res}} \rightarrow \frac{20A(\zeta, W^2)}{3(n_f + 4C_F)} \sum e_q^2 \left\{ 1 - \frac{87}{9} C_F \frac{\alpha_s(Q^2)}{4\pi} \right\}. \quad (29)$$

This expression coincides with the corresponding result from [19]² and can be readily obtained within the standard approach employing the 2π asymptotic GDA's. The asymptotic limit of the amplitude $[T_2(Q^2, \zeta, W^2)]^{\text{res}}$, due to the factor $D(Q^2)$, is equal to zero.

This analysis of the asymptotic limit of the Borel resummed amplitudes shows the internal consistency of the RC method itself.

¹ Below, for brevity, we do not write down explicitly the higher twist ambiguities in the resummed expressions.

² Our definition of the function $A(\zeta, W^2)$ differs by a factor $-1/6$ from that of [19].

4 Numerical results

Let us now present numerical estimates of the power corrections to the amplitudes. The resummed amplitude $[T_0(Q^2, \zeta, W^2)]^{\text{res}}$, which contains both the hard perturbative component and power corrections, can be rewritten in the form

$$[T_0(Q^2, \zeta, W^2)]^{\text{res}} = T_0^{\text{LO}}(Q^2, \zeta, W^2) + T_0^{\text{NLO}}(Q^2, \zeta, W^2) + T_0^{\text{PC}}(Q^2, \zeta, W^2), \quad (30)$$

where the first two terms in the RHS of (30) are the LO and NLO parts of the amplitude, whereas $T_0^{\text{PC}}(Q^2, \zeta, W^2)$ denotes the power corrections to it. The latter is given by the expression

$$T_0^{\text{PC}}(Q^2, \zeta, W^2) = [T_0(Q^2, \zeta, W^2)]_{\text{NLO}}^{\text{res}} - T_0^{\text{NLO}}(Q^2, \zeta, W^2). \quad (31)$$

For our purposes it is convenient to normalize the expressions (30) and (31) in terms of $T_0^{\text{LO}}(Q^2, \zeta, W^2)$, which results in ratios independent on the function $A(\zeta, W^2)$:

$$R(Q^2) = 1 + R_1(Q^2) + R_2(Q^2). \quad (32)$$

Here

$$R_1(Q^2) = \frac{T_0^{\text{NLO}}(Q^2, \zeta, W^2)}{T_0^{\text{LO}}(Q^2, \zeta, W^2)},$$

$$R_2(Q^2) = \frac{T_0^{\text{PC}}(Q^2, \zeta, W^2)}{T_0^{\text{LO}}(Q^2, \zeta, W^2)}. \quad (33)$$

In our calculations we use the following values of the parameters Λ and μ_0 :

$$\Lambda_4 = 0.2 \text{ GeV}, \quad \mu_0^2 = 1 \text{ GeV}^2. \quad (34)$$

To clarify the sensitivity of the predictions to the parameter $M_q(\mu_0^2)$ we shall take the two plausible values $M_q(1 \text{ GeV}^2) = 0.5$ and $M_q(1 \text{ GeV}^2) = 0.6$. We use the two-loop approximation for the QCD coupling $\alpha_s(Q^2)$.

The amplitude $[T_0(Q^2, \zeta, W^2)]^{\text{res}}$ contains an infinite number of IR renormalon poles. We truncate the corresponding series at some $n_{\text{max}} = 50$ which is amply sufficient [17, 18].

In Fig. 3 we show $R_2(Q^2)$ as a function of Q^2 . The power corrections amount to some 50–60 per cent of the corresponding leading order contribution at $Q^2 = 1 \text{ GeV}^2$. They are not completely negligible also at $Q^2 = 10 \text{ GeV}^2$ reaching around 15% of the LO term. One observes that in the region $1 \text{ GeV}^2 \leq Q^2 \leq 4 \text{ GeV}^2$ the function $R_2(Q^2)$ is more sensitive to the chosen value of the parameter M_q than in the domain $Q^2 \sim 10 \text{ GeV}^2$.

In Fig. 3 the ratios $R(Q^2)$, $1 + R_1(Q^2)$ are also shown. As is seen the power corrections significantly reduce the amplitude $T_0(Q^2, \zeta, W^2)$ and this effect depends on the 2π GDA used in calculations. Thus, at $Q^2 = 1 \text{ GeV}^2$ the resummed amplitude computed using the 2π GDA with the input parameter $M_q = 0.6$ is approximately twice as large as the same amplitude found employing the GDA

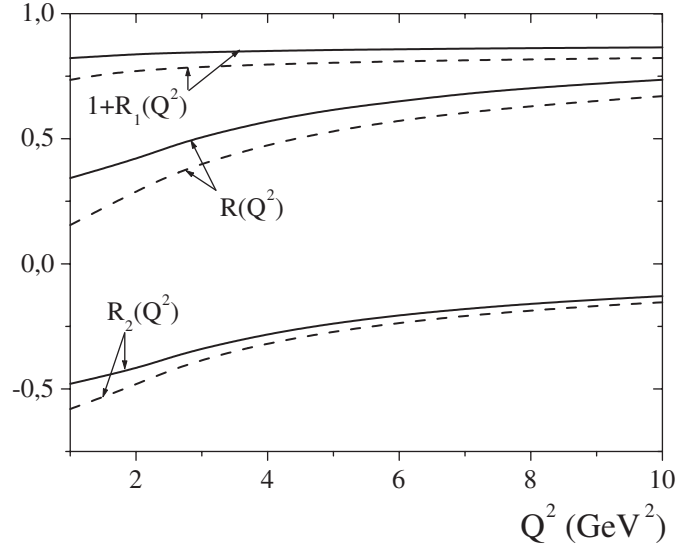


Fig. 3. The ratios $R_2(Q^2)$, $R(Q^2)$ and $1 + R_1(Q^2)$ as functions of Q^2 . The solid (dashed) curve corresponds to the parameter $M_q(1 \text{ GeV}^2) = 0.6$ [$M_q(1 \text{ GeV}^2) = 0.5$]

with $M_q = 0.5$. At the higher values of Q^2 this difference becomes more moderate, ~ 1.1 at $Q^2 = 10 \text{ GeV}^2$.

Another conclusion, which can be made after analysis of Fig. 3 is that the difference between the resummed [the ratio $R(Q^2)$] and the standard predictions for the amplitude [the ratio $1 + R_1(Q^2)$] becomes smaller at higher values of the momentum transfer Q^2 . In fact, at $Q^2 = 1 \text{ GeV}^2$ the resummed amplitude is equal to 0.41 of the standard result, whereas at 10 GeV^2 one gets 0.85 [for $M_q(1 \text{ GeV}^2) = 0.6$].

For phenomenological applications it is useful to parametrize the ratio $R_2(Q^2)$ using the power-suppressed terms $\sim 1/Q^{2n}$, $n = 1, 2, 3$. Our fitting procedure leads to the following expressions:

$$R_2(Q^2) \simeq \frac{1}{Q^2} \left[-1.709 + \frac{1.881}{Q^2} - \frac{0.7524}{Q^4} \right],$$

$$M_q(1 \text{ GeV}^2) = 0.5,$$

$$R_2(Q^2) \simeq \frac{1}{Q^2} \left[-1.462 + \frac{1.515}{Q^2} - \frac{0.533}{Q^4} \right],$$

$$M_q(1 \text{ GeV}^2) = 0.6. \quad (35)$$

The power corrections to the amplitude $T_2(Q^2, \zeta, W^2)$ are given by the formula

$$T_2^{\text{PC}}(Q^2, \zeta, W^2) = [T_2(Q^2, \zeta, W^2)]^{\text{res}} - T_2(Q^2, \zeta, W^2). \quad (36)$$

The ratio

$$R_3(Q^2) = \frac{T_2^{\text{PC}}(Q^2, \zeta, W^2)}{T_2(Q^2, \zeta, W^2)}$$

is shown in Fig. 4. It turns out that in this estimate the power corrections to the amplitude $T_2(Q^2, \zeta, W^2)$ are large

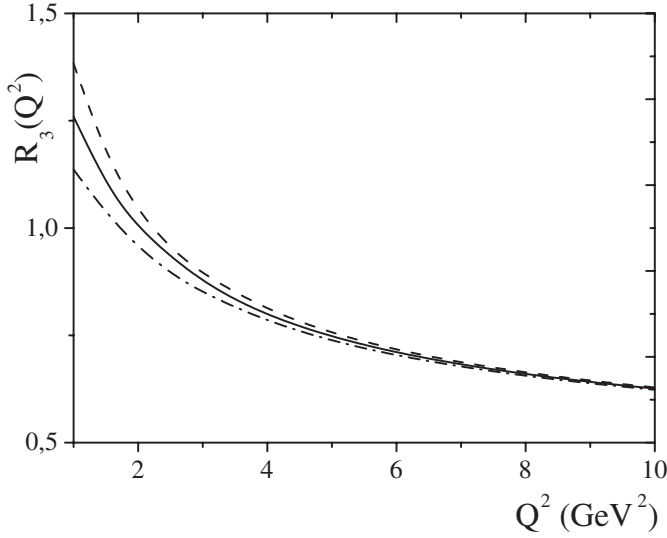


Fig. 4. The ratio $R_3(Q^2)$ versus Q^2 . The solid line corresponds to $R_3(Q^2)$ without the HT ambiguities. The broken lines are obtained by taking into account the HT ambiguities (18). For the dashed line: $N_2 = N_3 = 1$; for the dot-dashed line: $N_2 = N_3 = -1$

and may still amount to a 60 per cent increase of the amplitude at $Q^2 \sim 10 \text{ GeV}^2$. Such a large magnitude of the end-point effects can be traced back to the fact that $T_2(Q^2, \zeta, W^2)$ begins at $O(\alpha_S(Q^2))$. At the same time, the ratio of these power corrections to the total amplitude of the process remains within reasonable limits. To see this, we normalize the corrections T_2^{PC} in terms of the T_0^{LO} ignoring the different tensor factors in (4) and setting $A_g^T(\zeta, W^2) = A(\zeta, W^2)$, $D_g^T(1 \text{ GeV}^2) = 1$, but keeping the factor $\sum e_q^2$ in definition of the function $T_0(Q^2, \zeta, W^2)$. The ratio T_2^{PC}/T_0^{LO} calculated in this approximate way is shown in Fig. 5. We find that power corrections T_2^{PC} may amount to 31–38% of the T_0^{LO} at $Q^2 = 1 \text{ GeV}^2$ and only to 6–7% of its value at $Q^2 = 10 \text{ GeV}^2$. The precise estimate of the effects generated by the helicity-two component of the amplitude (4) requires more detailed investigation.

The HT ambiguities (18) coming from the principal value prescription, in the process under consideration are sizeable only for small values of the momentum transfer $1 \text{ GeV}^2 \leq Q^2 \leq 2.5 \text{ GeV}^2$ [from $\pm 9\%$ to $\pm 3\%$]. At $Q^2 = 5 \text{ GeV}^2$ they are already less than $\pm 1\%$ of the original result. As an example, the relevant curves for the ratio $R_3(Q^2)$ are shown in Fig. 4.

5 Concluding remarks

In this work we have estimated the power corrections to the amplitudes $T_i(Q^2, \zeta, W^2)$ of the process $\gamma^*\gamma \rightarrow \pi\pi$, originating from the end-point regions $z \rightarrow 0, 1$. To this end, we have employed the symmetrized RC method combined with techniques of the IR renormalon calculus. We have obtained the Borel resummed expressions $[T_i(Q^2, \zeta, W^2)]^{\text{res}}$ for the amplitudes and have removed IR

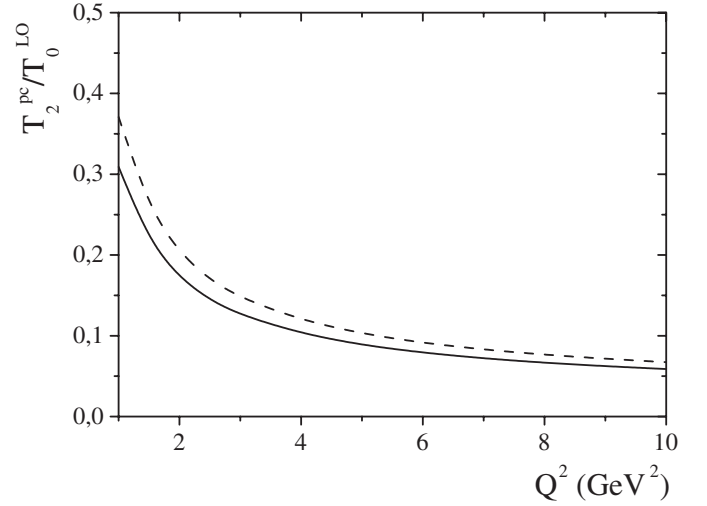


Fig. 5. The ratio T_2^{PC}/T_0^{LO} versus Q^2 . The solid (dashed) curve corresponds to the parameter $M_q(1 \text{ GeV}^2) = 0.6$ [$M_q(1 \text{ GeV}^2) = 0.5$]

renormalon divergences by means of a principal value prescription. In the considered process the Borel transform of the amplitude $T_0(Q^2, \zeta, W^2)$ contains an infinite number of the IR renormalon poles. Since each IR renormalon pole $u_0 = n$ in the Borel transforms $B_{q(g)}[T_0(Q^2, \zeta, W^2)](u)$, $B[T_2(Q^2, \zeta, W^2)](u)$ corresponds to the power correction $\sim 1/Q^{2n}$ to the amplitudes, and the expression (23), in general, contains power corrections $\sim 1/Q^{2n}$, $n = 1, 2, \dots, \infty$. In numerical computations we have truncated the corresponding series at $n_{\text{max}} = 50$. As an important consistency check, we have proved that the result obtained within the symmetrized RC method in the asymptotic limit $Q^2 \rightarrow \infty$ reproduces the standard prediction for the amplitudes.

It is known that the principal value prescription generates higher twist uncertainties. We have shown that these uncertainties at $Q^2 = 1 \text{ GeV}^2$ do not exceed $\pm 10\%$ of the original prediction and can be safely neglected in the region $Q^2 \geq 5 \text{ GeV}^2$.

Our numerical calculations have demonstrated in an admittedly method dependent way that the power corrections coming from the analysis of end-point regions may be essential in the region of photon virtualities $Q^2 \sim$ a few GeV^2 . Therefore, the phenomenological analysis of the process $\gamma^*\gamma \rightarrow \pi\pi$ in the presently experimentally-accessible energy regimes should include them.

Acknowledgements. We acknowledge useful discussions and correspondence with M. Diehl, G. Grunberg, L. Szymanowski and O.V. Teryaev. One of the authors (S.S.A.) would like to thank the members of the PHASE group for hospitality at IPN Orsay and gratefully to acknowledge the financial support from NATO Fellowship program.

References

1. G.P. Lepage, S.J. Brodsky, Phys. Rev. D **22**, 2157 (1980); A.V. Efremov, A.V. Radyushkin, Theor. Math. Phys. **42**, 97 (1980) [Teor. Mat. Fiz. **42**, 147 (1980)]; Phys. Lett. B **94**, 245 (1980); A. Duncan, A.H. Mueller, Phys. Rev. D **21**, 1636 (1980); V.L. Chernyak, A.R. Zhitnitsky, Phys. Rep. **112**, 173 (1984)
2. M. Diehl, T. Gousset, B. Pire, O. Teryaev, Phys. Rev. Lett. **81**, 1782 (1998); M. Diehl, T. Gousset, B. Pire, Phys. Rev. D **62**, 073014 (2000); A. Freund, Phys. Rev. D **61**, 074010 (2000); I.V. Anikin, B. Pire, O.V. Teryaev, Phys. Rev. D **69**, 014018 (2004)
3. O.V. Teryaev, Phys. Lett. B **510**, 125 (2001)
4. X. Ji, Phys. Rev. Lett. **78**, 610 (1997); Phys. Rev. D **55**, 7114 (1997); A.V. Radyushkin, Phys. Lett. B **380**, 417 (1996); Phys. Rev. D **56**, 5524 (1997)
5. M. Diehl, Phys. Rept. **388**, 41 (2003)
6. B. Pire, L. Szymanowski, Phys. Lett. B **556**, 129 (2003)
7. P. Achard et al. [L3 Collaboration], Phys. Lett. B **568**, 11 (2003); D. Urner, AIP Conf. Proc. **698**, 566 (2004) [hep-ex/0309045]
8. M. Vanderhaeghen, P.A.M. Guichon, M. Guidal, Phys. Rev. D **60**, 094017 (1999)
9. N. Kivel, L. Mankiewicz, Eur. Phys. J. C **18**, 107 (2000)
10. N. Kivel, L. Mankiewicz, Phys. Rev. D **63**, 054017 (2001); I.V. Anikin, O.V. Teryaev, Phys. Lett. B **509**, 95 (2001)
11. S.J. Brodsky, G.P. Lepage, P.B. Mackenzie, Phys. Rev. D **28**, 228 (1983)
12. E. Braaten, Y.-Q. Chen, Phys. Rev. D **57**, 4236 (1998) [Erratum D **59**, 079901 (1999)]; R. Akhoury, A. Sinkovics, M.G. Sotiropoulos, Phys. Rev. D **58**, 013011 (1998); A.V. Belitsky, A. Schäfer, Nucl. Phys. B **527**, 235 (1998); J. Andersen, Phys. Lett. B **475**, 141 (2000); E. Gardi, G. Grunberg, JHEP **9911**, 016 (1999); A. Belitsky, AIP Conf. Proc. **698**, 607 (2004) [hep-ph/0307256]; V.M. Braun, E. Gardi, S. Gottwald, Nucl. Phys. B **685**, 171 (2004)
13. M. Beneke, Phys. Rep. **317**, 1 (1999); A. Grozin, hep-ph/0311050
14. S.S. Agaev, Phys. Lett. B **360**, 117 (1995) [Erratum B **369**, 379 (1996)]; Mod. Phys. Lett. A **10**, 2009 (1995)
15. S.S. Agaev, Mod. Phys. Lett. A **11**, 957 (1996); A **13**, 2637 (1998); Eur. Phys. J. C **1**, 321 (1998); Few Body Syst. Suppl. **11**, 263 (1999); Nucl. Phys. B (Proc. Suppl.) **74**, 155 (1999); S.S. Agaev, A.I. Mukhtarov, Y.V. Mamedova, Mod. Phys. Lett. A **15**, 1419 (2000); S.S. Agaev, A.I. Mukhtarov, Int. J. Mod. Phys. A **16**, 3179 (2001); A.I. Karanikas, N.G. Stefanis, Phys. Lett. B **504**, 225 (2001)
16. S.S. Agaev, Phys. Rev. D **64**, 014007 (2001)
17. S.S. Agaev, Phys. Rev. D **69**, 094010 (2004)
18. S.S. Agaev, N.G. Stefanis, Eur. Phys. J. C **32**, 507 (2004)
19. N. Kivel, L. Mankiewicz, M.V. Polyakov, Phys. Lett. B **467**, 263 (1999)
20. M.V. Polyakov, Nucl. Phys. B **555**, 231 (1999); Ph. Hägler, P. Pire, L. Szymanowski, O.V. Teryaev, Phys. Lett. B **535**, 117 (2002) [Erratum B **540**, 324 (2002)]; Eur. Phys. J. C **26**, 261 (2002)
21. H. Contopanagos, G. Sterman, Nucl. Phys. B **419**, 77 (1994)
22. G. 't Hooft, in Whys of Subnuclear Physics, Proceeding of the International School, Erice, 1977, edited by A. Zichichi (Plenum, New York 1978); A.I. Zakharov, Nucl. Phys. B **385**, 452 (1992)